

CHEM MED CHEM

CHEMISTRY ENABLING DRUG DISCOVERY

Accepted Article

Title: Halogenated bis(methoxy-benzylidene)-4-piperidone curcuminoids with improved anticancer activity

Authors: Florian Schmitt, Dharmalingam Subramaniam, Shrikant Anant, Subhash Padhye, Gerrit Begemann, Rainer Schobert, and Bernhard Biersack

This manuscript has been accepted after peer review and appears as an Accepted Article online prior to editing, proofing, and formal publication of the final Version of Record (VoR). This work is currently citable by using the Digital Object Identifier (DOI) given below. The VoR will be published online in Early View as soon as possible and may be different to this Accepted Article as a result of editing. Readers should obtain the VoR from the journal website shown below when it is published to ensure accuracy of information. The authors are responsible for the content of this Accepted Article.

To be cited as: *ChemMedChem* 10.1002/cmdc.201800135

Link to VoR: <http://dx.doi.org/10.1002/cmdc.201800135>

WILEY-VCH

www.chemmedchem.org

A Journal of



FULL PAPER

Halogenated bis(methoxy-benzylidene)-4-piperidone curcuminoids with improved anticancer activity

Florian Schmitt,^[a] Dharmalingam Subramaniam,^[b] Shrikant Anant,^[b] Subhash Padhye,^[b] Gerrit Begemann,^[c] Rainer Schobert,^[a] Bernhard Biersack*^[a]

[a] F. Schmitt, Prof. Dr. R. Schobert, Dr. B. Biersack
Department of Chemistry
University of Bayreuth
Universitätsstraße 30, 95440 Bayreuth (Germany)
E-mail: bernhard.biersack@yahoo.de

[b] Prof. Dr. D. Subramaniam, Prof. Dr. S. Anant, Prof. Dr. S. Padhye
University of Kansas Medical Center
3901 Rainbow Boulevard, Kansas City 66160 (USA)

[c] Prof. Dr. G. Begemann
Developmental Biology
University of Bayreuth
Universitätsstraße 30, 95440 Bayreuth (Germany)

Abstract: A series of readily available curcuminoids **3a-f** with halogenated bis(4-methoxy/4,5-dimethoxybenzylidene)-4-piperidone structure was prepared and analyzed for their cytotoxic impact on eight human cancer cell lines of five different entities. The known 3,4,5-trimethoxybenzylidene curcuminoid **2a** and the new bis-(3-bromophenyl)- and bis-(3,5-dibromophenyl)-derivatives **3c** and **3d** proved more strongly antiproliferative than the known curcuminoid EF24 against six of these cell lines. Compounds **2a** and **3c** caused a distinct increase of reactive oxygen species, which eventually elicited apoptosis in 518A2 melanoma cells. **2a** arrested 518A2 melanoma cells in G1 phase of the cell cycle and had no effect on the expression of prometastatic matrix metalloproteinases MMP-2 and MMP-9, whereas **3c** led to an accumulation of 518A2 cells in G2/M phase and to a down-regulation of the MMP-2 expression. In addition, **2a** and **3c** treatment resulted in significant inhibition of colony formation in HCT-116 cells. Both **2a** and **3c** showed antiangiogenic activity, e.g. by inhibiting the formation of subintestinal veins (SIV) in zebrafish embryos. **3c** was also well-tolerated by mice and inhibited the growth of HCT-116 colon cancer xenografts.

Introduction

EF24 was originally synthesized as a mono-carbonyl derivative of curcumin, a natural polyphenol extracted from the rhizome of the plant *Curcuma longa* (Fig. 1). There is ample literature classifying curcumin as a multi-potent anticancer agent but also controversial discussions as to whether its application is meaningful and effective given its poor water solubility, its rapid metabolic degradation, and its consequently low bioavailability in plasma and tissue.^[1,2] When compared to curcumin, its mono-carbonyl analog EF24 showed improved metabolic stability and uptake, causing a distinctly increased bioavailability.^[3] Moreover, the anticancer potential of EF24 exceeded that of curcumin by far. EF24 restricts cell proliferation and induces apoptosis via the intrinsic pathway and as a consequence of an enhanced reactive oxygen species (ROS) production as it was presented for curcumin before.^[4-9] In addition, EF24 was shown to reduce the cell motility^[10] and to exert antiangiogenic activity.^[11] Moreover, several other cancer-relevant targets are addressed by EF24 as

demonstrated by its inhibition or down-regulation of NF- κ B,^[5] COX-2,^[6,12] STAT-3, Akt,^[12] and MMP-2^[13]. Apart from EF24, a multiplicity of mono-carbonyl analogs of curcumin were synthesized and investigated including bis(arylidene) derivatives of acetone, cycloalkanones, piperidones, and tetrahydro-4H-(thio)pyran-4-ones.^[14-22] Recently, our group reported on several mono-carbonyl curcumin analogs with different fluoro and pentafluorothio substituents on the phenyl rings, which showed antiproliferative, antiangiogenic and vascular-disruptive activity.^[23] Since curcuminoids with a piperidin-4-one backbone displayed the highest cytotoxicities against cancer cells, we now kept this backbone unaltered and concentrated on the modification of the phenyl rings starting with the 3,4,5-trimethoxyphenyl motif of the lead compound **2a** (Scheme 1). This 3,4,5-trimethoxyphenyl motif was observed in many biologically active compounds, such as combretastatin A-4, podophyllotoxin and colchicine,^[24-26] as well as in highly active synthetic curcuminoids.^[27-29] Even though compound **2a** has been known for years, it has up to now only been tested against leukemia, glioblastoma and laryngeal carcinoma cell lines.^[30-32] In the present paper, we investigate its antiproliferative effect on cancer cells of other entities as well as its impact on other cancer-relevant parameters such as ROS production, cell cycle progression, angiogenesis, and the expression of matrix-metalloproteinases MMP-2 and MMP-9. Since our group had previously disclosed 3-halo/3,5-dihalo-4,5-dimethoxyphenyl-imidazoles with anticancer activities exceeding that of combretastatin A-4 in resistant cancer cell lines^[33,34], we also synthesized a series of halogenated bis(methoxy-benzylidene)-4-piperidones and evaluated the influence of halogenation on their anticancer activities in comparison to **2a**.

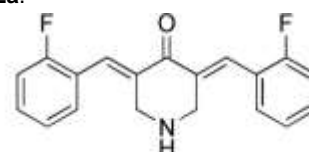
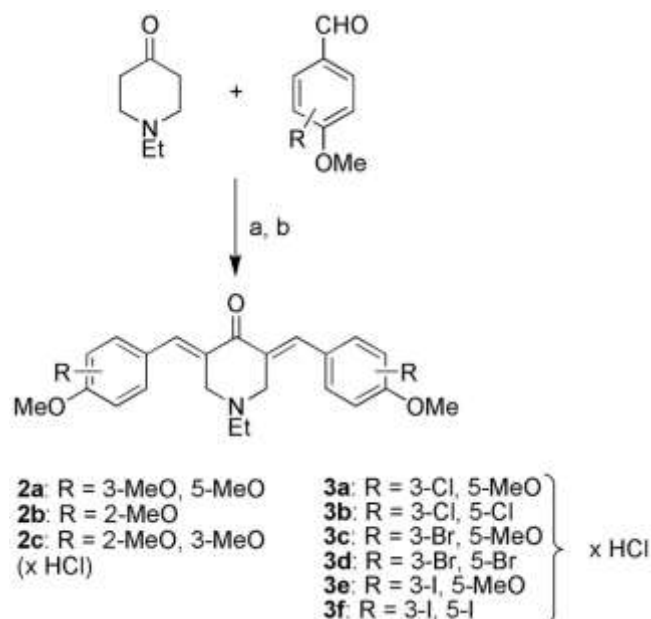


Figure 1. Structure of the mono-carbonyl curcumin analog EF24.

Results and Discussion

FULL PAPER

Curcuminoid **2a** and the new derivatives **2b-c** and **3a-f** were prepared by condensation of 1-ethyl-4-piperidone (**1**) with the corresponding benzaldehydes under basic conditions (Scheme 1). In most cases (**2c**, **3a-f**) treatment with HCl/dioxane and crystallisation of the curcuminoids as hydrochloride salts was necessary in order to obtain the pure target compounds as yellow solids. The logP values of the compounds (free bases) were compared with that of EF24 and **2a-c** were calculated to be more hydrophilic than EF24 (Tab. S1, cf. Supplementary Data). In addition, **3a** and **3c** revealed logP below 5 and, thus, did not violate Lipinski rule.



Scheme 1. Synthesis of the curcuminoids **2a-c** and their halogenated analogs **3a-f**. Reagents and conditions: a) NaOH, MeOH, rt; b) 4 M HCl/dioxane, CH₂Cl₂, rt for **2c**, **3a-f**.

Biological evaluation

Antiproliferative activity.

The antiproliferative activity of compounds **2a-c**, **3a**, and **3c-f** was evaluated by MTT [3-(4,5-dimethylthiazol-2-yl)-2,5-diphenyltetrazolium bromide] assays against seven human cancer cell lines of five different entities (Table 1).^[35] **3b** was not

soluble in EtOH or DMSO at concentrations suitable for this assay. All tested curcuminoids showed dose-dependent inhibition curves with IC₅₀ values ranging from triple-digit nanomolar to single-digit micromolar. In the row of curcuminoids substituted with methoxy groups only, the known bis-3,4,5-trimethoxyphenyl curcuminoid **2a** performed best. The effect of the corresponding 2,4-dimethoxy substituted analog **2b** was distinctly weaker followed by the 2,3,4-trimethoxy substituted compound **2c** which was the least active compound in this series. The introduction of halogen substituents at the phenyl rings led to distinct changes in the cytotoxicities of the new compounds **3a**, and **3c-f**. The bis-3-chloro-4,5-dimethoxyphenyl substituted **3a** and the bis-3-iodo-4,5-dimethoxyphenyl compound **3e** were slightly less active when compared to **2a** whereas in case of **3f** a distinct drop in activity was observed. The introduction of bromine substituents at the phenyl rings turned out to have the best effect on the cytotoxicities of the test compounds **3c** and **3d**. On average, the bis-3,5-dibromo-4-methoxyphenyl curcuminoid **3d** was about as active as the lead compound **2a** whereas the bis-3-bromo-4,5-dimethoxyphenyl **3c** was more active even when compared to **2a**. It has to be emphasized that the antiproliferative activity of the bromo derivatives **3c** and **3d** as well as that of **2a** exceeded even that of the well-investigated curcuminoid EF24.^[23]

However, there was no specificity for a certain cancer cell line except for the multidrug resistant MCF-7^{Topo} breast carcinoma, being on average less sensitive to the test compounds. Interestingly, **3f** is about eight times less efficacious against MCF-7^{Topo} than against the other cell lines. It can be assumed that **3d** is a substrate of the ABC (ATP binding cassette) efflux transporter BCRP (breast cancer resistance protein) which is overexpressed in MCF-7^{Topo} cells.

The structure-activity relationships observed in these MTT assays were confirmed in hexoseaminidase enzyme assays with SW-480 and HCT-116 colon carcinoma cells which took stock of the time-dependency of the cytotoxicities (Table 2).^[36] Compounds **3a-c** as well as **2a** strongly inhibited the growth of HCT-116 cells yet after 24 h, whereas **2b-c** and **3d-f** showed a delayed and overall weaker effect. The SW-480 cancer cell line appeared to be slightly less sensitive to the active test compounds when compared with the HCT-116 cancer cell line. After 72 h both cell lines had responded well to compounds **2a** and **3a-c** which displayed excellent IC₅₀ values in the range of 0.2-0.3 μM.

Table 1. Inhibitory concentrations IC₅₀^[a] [μM] of **2a-c**, **3a**, **3c-f** and EF24^[b] when applied to cells of human 518A2 melanoma, KB-V1^[b] cervix carcinoma, Panc-1 pancreatic ductular adenocarcinoma, MCF-7^{Topo} breast carcinoma and HT-29, HCT-116 and DLD-1 colon (adeno-)carcinomas

	518A2	HT-29	HCT-116	DLD-1	KB-V1 ^[b]	MCF-7 ^{Topo}	Panc-1
2a	0.65 ± 0.03	0.89 ± 0.05	0.65 ± 0.03	1.0 ± 0.1	0.61 ± 0.06	1.6 ± 0.2	0.90 ± 0.08
2b	1.8 ± 0.2	1.9 ± 0.2	1.3 ± 0.1	2.2 ± 0.2	1.1 ± 0.1	2.9 ± 0.2	2.2 ± 0.1
2c	5.7 ± 0.3	3.4 ± 0.1	2.7 ± 0.2	1.8 ± 0.1	1.8 ± 0.1	3.7 ± 0.2	2.3 ± 0.2
3a	0.83 ± 0.08	1.8 ± 0.2	0.89 ± 0.06	1.1 ± 0.1	1.3 ± 0.1	3.2 ± 0.2	1.8 ± 0.1
3c	0.55 ± 0.03	0.95 ± 0.03	0.78 ± 0.02	0.40 ± 0.05	0.54 ± 0.06	0.95 ± 0.05	0.73 ± 0.05
3d	0.49 ± 0.04	0.93 ± 0.02	0.35 ± 0.02	1.2 ± 0.1	0.43 ± 0.01	1.3 ± 0.1	1.7 ± 0.1
3e	3.6 ± 0.2	0.62 ± 0.05	0.73 ± 0.08	0.70 ± 0.03	1.0 ± 0.1	3.0 ± 0.4	1.3 ± 0.1
3f	3.3 ± 0.4	5.5 ± 0.3	1.8 ± 0.1	1.9 ± 0.1	3.5 ± 0.3	22 ± 2	2.2 ± 0.1
EF24 ^[b]	1.8 ± 0.2	1.6 ± 0.1	1.5 ± 0.2	1.3 ± 0.1	1.1 ± 0.1	2.2 ± 0.2	1.5 ± 0.2

[a] Values are the means ± SD (standard deviation) of four independent experiments. They were derived from concentration–response curves obtained by measuring the percentage of vital cells relative to untreated controls after 72 h using MTT-assay. [b] Values of EF24 were taken from ref. [21].

FULL PAPER

Table 2. Inhibitory concentrations IC₅₀^[a] [μM] of **2a-c** and **3a-f** when applied to cells of human HCT-116 and SW-480 colon carcinomas

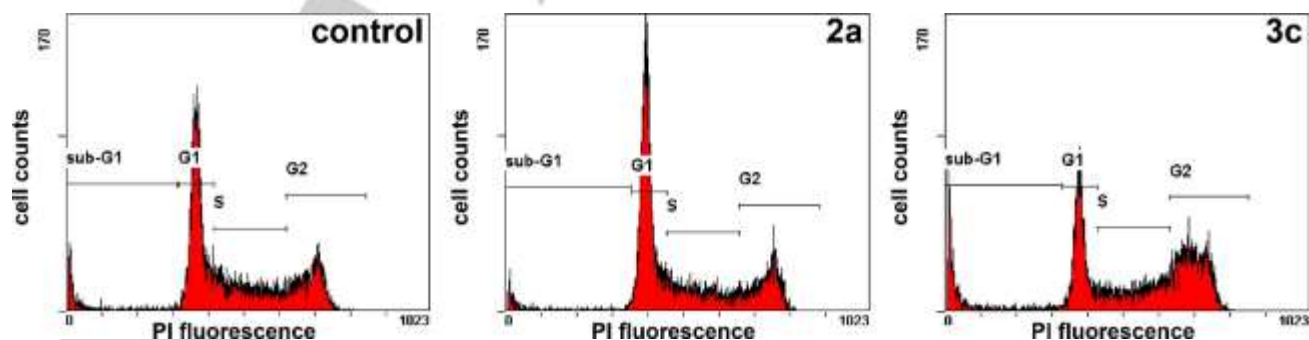
	HCT-116			SW-480		
	24 h	48 h	72 h	24 h	48 h	72 h
2a	0.5	0.3	0.3	1.0	0.4	0.3
2b	8.0	4.0	3.0	>10	>10	4.0
2c	>10	5.0	1.0	>10	4.0	3.0
3a	0.4	0.3	0.25	0.5	0.3	0.25
3b	0.4	0.3	0.25	1.0	0.4	0.25
3c	0.4	0.3	0.2	0.7	0.3	0.25
3d	1.2	0.5	0.3	2.0	0.5	0.3
3e	1.0	0.6	0.6	2.0	0.5	0.5
3f	>10	3.8	2.0	>10	>10	4.0

[a] Values are derived from concentration–response curves obtained by measuring the percentage of vital cells relative to untreated controls after 24 h, 48 h, and 72 h using hexoseaminidase assay. Values represent the mean (SD ± 15%) of two independent experiments.

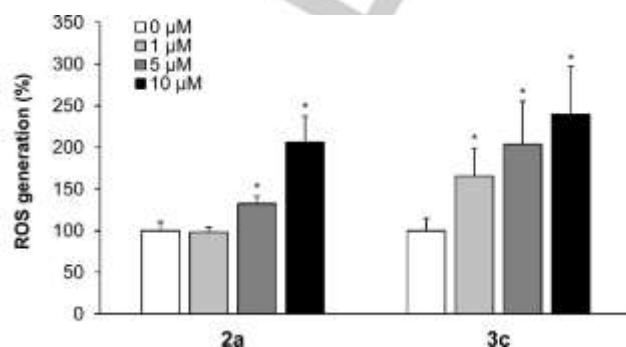
Analogous tests of **2a** and **3c** against non-malignant FHC colon epithelial cells revealed a ca. two-fold lower activity in the FHC cells (IC₅₀ ca. 0.5 μM after 48 h) when compared with their activity against HCT-116 and SW-480 colon cancer cells (*cf.* Supplementary Data).

Effect on intracellular ROS levels.

The compound-induced ROS generation has been recognized as one of the mechanisms underlying the cytotoxicity of compounds since the ROS overproduction induces ER (endoplasmic reticulum) stress and mitochondrial apoptosis.^[37] Curcuminoids such as EF24 are known to affect the ROS production and as a consequence induce apoptosis in cancer cells.^[38] Therefore, we investigated the effect of **2a** and **3c** on the intracellular ROS levels in 518A2 melanoma cells using the DCFH-DA (2',7'-dichlorohydrofluorescein diacetate) assay. After cellular uptake, DCFH-DA is deacetylated by cellular esterases to DCFH (2',7'-dichlorohydrofluorescein). Then, DCFH is oxidized by ROS to the fluorescent DCF (2',7'-dichlorofluorescein). Hence, its fluorescence intensity is proportional to the intracellular ROS levels. Both test compounds, **2a** and **3c**, caused an increase of the cellular ROS levels exceeding 200% at 10 μM compared to that of untreated control cells which was set to 100% (Fig. 2).

**Figure 3.** Effect of **2a** (800 nM), **3c** (600 nM) and control (DMSO) on the cell cycle progression of 518A2 melanoma cells after 24 h exposure. The cell cycle profiles are representative of three independent experiments obtained by flow cytometry after PI staining.

Even at concentrations as low as 1 μM the relative ROS production in cells treated with **3c** exceeded 150% whereas the treatment with **2a** left the cellular ROS levels unaltered. The rapid increase of ROS is probably causative for the strong antiproliferative effects of **2a** and **3c** after 24 h and possibly also for the arrest of cells in cell cycle progression and for apoptosis.

**Figure 2.** ROS generation in 518A2 melanoma cells induced by test compounds **2a** and **3c**. After the pretreatment of the cells with DCFH-DA (20 μM, 30 min), the cells were incubated with the test compounds **2a** and **3c** (0, 1, 5, and 10 μM; 1 h). The green fluorescence of DCF as a measure of the intracellular ROS level was set to 100% for vehicle treated control cells (0 μM). The ROS generation (%) is depicted as the mean ± SD of five independent experiments. Significant deviations from control data were determined using a t-test. *: p < 0.002.

Cell cycle analysis.

The effect of the test compounds **2a** (800 nM) and **3c** (600 nM) on the cell cycle progression in 518A2 melanoma cells was assessed after staining the DNA with propidium iodide (PI) by using flow cytometry (Fig. 3; Table 3). The treatment of the cells with bis-3,4,5-trimethoxyphenyl derivative **2a** caused a distinct increase of cells in G1 phase, whereas the percentage of cells in S and G2/M phase was reduced. The change in the proportion of apoptotic sub-G1 cells was negligible. In contrast to that, compound **3c** caused a significant accumulation of cells in G2/M phase of the cell cycle. The percentages of cells in G1 and S were decreased whereas the treatment with **3c** gave rise to an increase of apoptotic sub-G1 events.

FULL PAPER

Table 3. Effect of **2a** (800 nM) and **3c** (600 nM) on the cell-cycle progression of 518A2 melanoma cells. Percentages of cells in G1, S and G2/M phase of the cell cycle as well as the proportion of apoptotic sub-G1 cells as obtained by flow cytometry after DNA staining with PI are depicted as the means \pm SD of three independent experiments. Control: DMSO.

	sub-G1	G1	S	G2/M
control	5.9 \pm 1.4	42.2 \pm 1.2	27.1 \pm 0.6	24.8 \pm 1.9
2a	6.2 \pm 0.9	49.4 \pm 2.2	22.5 \pm 0.1	21.9 \pm 1.2
3c	11.7 \pm 2.4	31.7 \pm 4.2	22.5 \pm 1.8	34.1 \pm 1.9

Effects on matrix metalloproteinases.

Matrix metalloproteinases (MMPs) are zinc-dependent endopeptidases which are expressed and secreted at high concentrations especially by invasive tumor cells and vascular endothelial cells.^[39,40] They mediate the proteolytic degradation of the extracellular matrix (ECM) so that endothelial or tumor cells can egress from or invade into tissues which is a requirement for tumor angiogenesis or metastasis.^[40,41] The essential role of MMPs in tumor progression is widely recognized so that MMPs are a promising anticancer target. Since gelatin is a substrate of MMP-2 and MMP-9, the test compounds' effects on expression and secretion of them in 518A2 melanoma cells could simply be tested by gelatin zymography.^[42] Since it is known that curcuminoids such as EF24^[13], Y20^[43] and curcumin^[44] (*cf.* Supplementary Data) inhibit the production of MMP-2, the effect of **2a** and **3c** on the intracellular and extracellular levels of MMP-2 in 518A2 melanoma cells was tested (Fig. 4, *cf.* Supplementary Data). Both test compounds **2a** and **3c** had virtually no effect on the cellular and extracellular levels of MMP-9. Moreover, **2a** did not alter these levels for MMP-2, either. In contrast, **3c** significantly reduced the levels of MMP-2 in cell medium and lysate, so that it can be assumed that the treatment with **3c** reduces the expression of MMP-2.

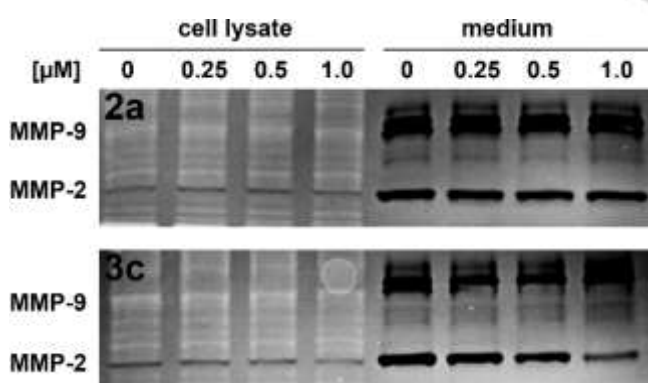


Figure 4. Effect of **2a** and **3c** (0, 0.25, 0.5 and 1 μ M) on the cell-associated and secreted activities of MMP-2 and MMP-9 in 518A2 melanoma cells after 24 h exposure. Cell lysate and media probes were subjected to gelatin zymography. Control (DMSO) treated probes are listed as 0 μ M. Images are representative of two independent experiments (negative images of the gelatin gels).

Effects on colony formation of cancer cells.

In order to evaluate the long-term effects of **2a** and **3c**, HCT-116 colon cancer cells were incubated with **2a** or **3c** for 48 h. Then,

the treated cells were allowed to grow in normal medium for 10 days in order to grow colonies. Both **2a** and **3c** strongly suppressed colony formation in colon cancer cells (Fig. 5). These results suggest that the anticancer effects of **2a** and **3c** are long-lasting and irreversible.

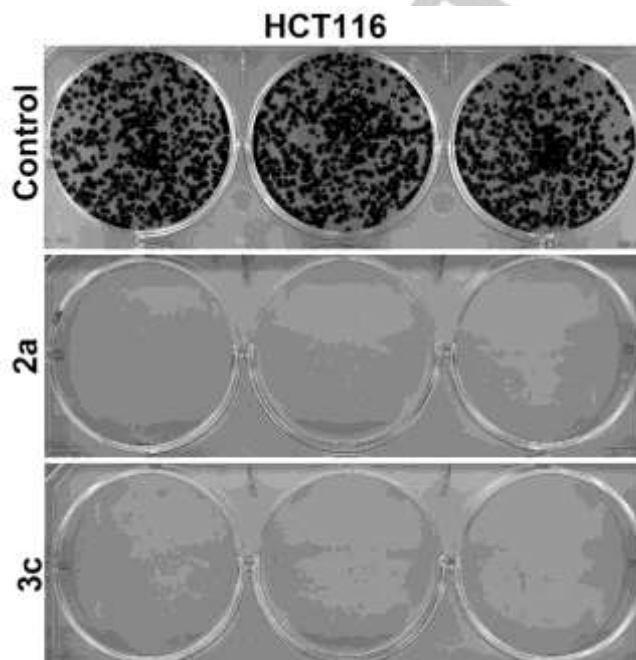


Figure 5. Compounds **2a** and **3c** inhibit colony formation. HCT-116 colon cancer cells were incubated with 0.5 μ M **2a** or **3c** for 48 h and allowed to grow and form colonies for 10 days. Control probes were treated with DMSO. Results are representative of three independent experiments.

Antiangiogenic effect.

The zebrafish (*Danio rerio*) is a commonly used vertebrate model to study the effect of test substances on angiogenesis since its circulatory system and its development is quite similar to that of mammals. The development of the subintestinal veins (SIVs) was used as a marker for angiogenesis.^[45] 48 hours past fertilization (hpf) they begin to develop from the common cardinal veins and form a network across the yolk of the embryos.^[46] At a later stage, the SIVs provide the blood supply for the digestive system. Embryos of the line *Tg(fli1a:EGFP)* crossed into a background of the unpigmented *casper* mutant, were used to monitor fluorescence of the EGFP-positive blood vessels (EGFP, enhanced green fluorescence protein).^[47,48] The area covered by SIVs of at least 17 identically treated embryos was then quantified and compared with that of vehicle treated control embryos, which was set to 100% SIV area (Fig. 6). Both, **2a** and **3c** showed a significant reduction of the SIV area to 74% \pm 13 and 81% \pm 17, respectively.

FULL PAPER

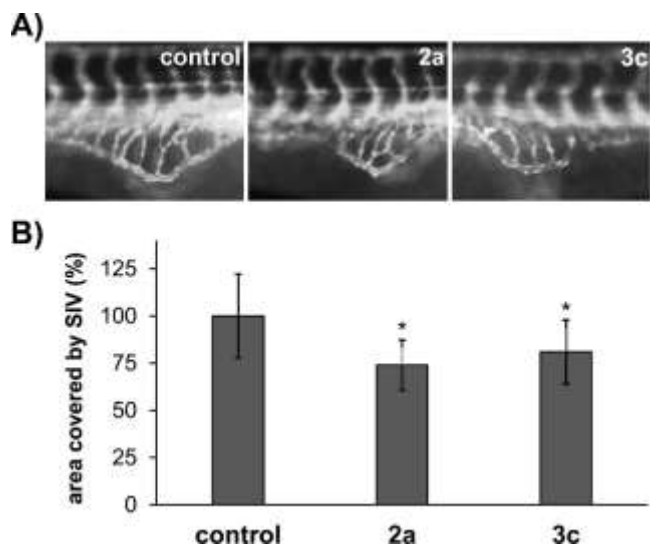


Figure 6. Antiangiogenic effect of test compound **2a** and **3c** in zebrafish embryos. Dechorionated 24 hpf old transgenic *Tg(fli1a:EGFP)* zebrafish with a *casper* background were treated with 5 μ M of the test compounds or vehicle (DMSO) for 48 h at 28 °C in embryo medium. A) Images are representative of at least 17 identically treated embryos (6.3-fold magnification). B) The area covered by subintestinal veins (SIV) was quantified by using the imageJ software. Values are the means \pm SD of at least 17 independent experiments with the SIV area of vehicle (DMSO) treated embryos set to 100%. Significant deviations from the control data were determined using a t-test. *: $p < 0.01$.

Inhibition of HCT-116 tumor xenograft growth.

To evaluate the effect of **3c** on tumor growth *in vivo*, we next examined its effects on growth of HCT116 induced xenografts. Colon cancer xenografts were allowed to develop and grow for one week before **3c** was administered intraperitoneally daily for three weeks. **3c** inhibited the growth of tumor xenografts, (Fig. 7B). The excised tumors from control animals weighed ~1200 mg, those treated with **3c** weighed ~250 mg (Fig. 7C&D). In addition, tumor volume was significantly decreased (Fig. 7B). There was no apparent change in liver, spleen, or body weight in the animals (data not shown). The treated mice were apparently in relatively good condition (*cf.* Supplementary Data). These *in vivo* results demonstrate that **3c** is a potential therapeutic agent for treating colon cancer while being relatively non-toxic to the animals.

Conclusions

A series of halogenated bis(4-methoxy/4,5-dimethoxybenzylidene)-4-piperidones **3a-f** was synthesized as new derivatives of the known trimethoxy curcuminoid **2a**. The antitumoral properties of compound **2a** which was up to now only tested in leukemia and glioblastoma cells lines, were investigated in more detail. The effect of halogenation on their anticancer effects was evaluated for **3a-f**. Compound **2a** as well as the 3-bromo compound **3c** and the 3,5-dibromo analog **3d**, showed superior antiproliferative activities against seven cancer cell lines when compared to the extensively investigated curcuminoid EF24. The new compound **3c** in particular exhibited a greater antiproliferative effect than **2a** on five of the seven cancer cell lines including the multi-drug resistant cancer cell lines MCF-7^{Topo} and KB-V1^{Vbl} which overexpress the ABC efflux transporters BCRP

and P-gp (P-glycoprotein), respectively. The 3-iodo and 3,5-diiodo substituted curcuminoids **3e** and **3f** were significantly less active, possibly because of the large iodo substituents posing a steric hindrance. The cytotoxicity of **2a** and **3c** is probably a consequence of them increasing the intracellular ROS concentration, which eventually causes apoptosis induction. Compound **3c** led to a rise of the intracellular ROS levels at distinctly lower concentrations compared to the parent compound **2a**. Both curcuminoids, **2a** and **3c**, showed significant antiangiogenic activity *in vivo* in zebrafish embryos, yet only **3c** inhibited the expression of the angiogenesis- and motility-relevant matrix metalloproteinase MMP-2 in 518A2 melanoma cells. The combination of its antiangiogenic and anti-migratory effects highlights the great potential of **3c** as a new anticancer drug candidate, which is underlined by the strong inhibition of colorectal tumors in mice by non-toxic doses of **3c**.

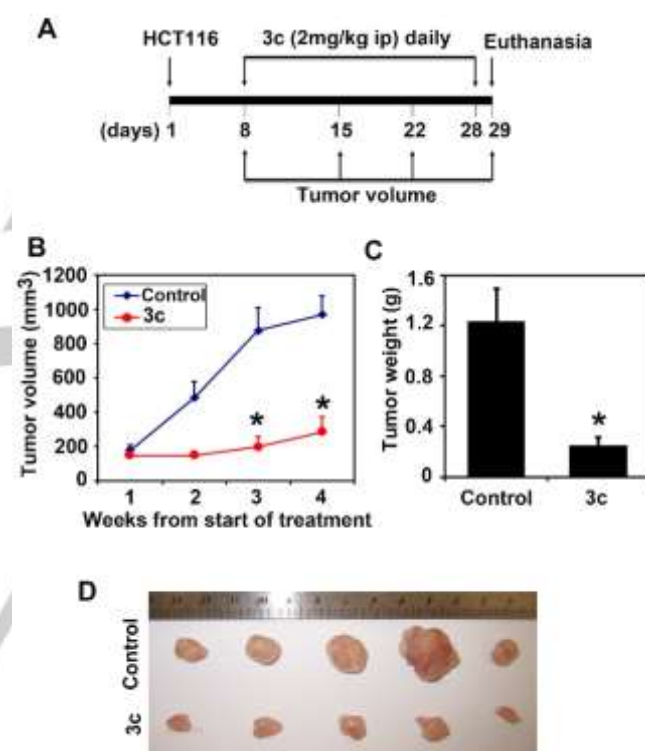


Figure 7. **3c** inhibits HCT116 induced tumor xenograft growth. (A) Experimental plan, (B) HCT116 cells were injected in to the flanks of nude mice and palpable tumors were allowed to develop for 7 days. Subsequently, **3c** (2 mg/kg bw) was injected daily intraperitoneally every day for 21 days. Tumor size was measured every week. On day 22, tumors were excised and subject to further analyses. Tumor volumes of **3c** treated mice were smaller when compared to control (* $p < 0.05$). C and D. **3c** treatment significantly reduced the tumor weight and size when compared to control.

Experimental Section

Chemistry

General: Starting materials and reagents were purchased from Sigma-Aldrich. The known compounds EF24 and **2a** were synthesized according to literature procedures.^[49,50] The following instruments were used: melting points (uncorrected), Gallenkamp; IR spectra, Perkin-Elmer Spectrum One

FULL PAPER

FT-IR spectrophotometer with ATR sampling unit; nuclear magnetic resonance spectra, BRUKER Avance 300 spectrometer; chemical shifts are given in parts per million (d) downfield from tetramethylsilane as internal standard; mass spectra, Varian MAT 311A (EI); microanalyses, Perkin-Elmer 2400 CHN elemental analyzer. All tested compounds were >95% pure by elemental analysis.

Synthesis of compounds 2b-c, 3a-f: (*E*)-1-Ethyl-3,5-bis(2,4-dimethoxybenzylidene)-4-piperidone (**2b**). 1-Ethyl-4-piperidone (95 mg, 0.75 mmol) was dissolved in MeOH (5 mL) and 2,4-dimethoxybenzaldehyde (249 mg, 1.5 mmol) was added. NaOH (40 mg, 1 mmol) and H₂O (1 mL) were added and the reaction mixture was stirred at room temperature for 16 h. The formed precipitate was collected, washed with MeOH and dried in vacuum which gave compound **2b** as a yellow solid (120 mg, 37%): mp: 127–128°C; ¹H NMR (300 MHz, [D₆]DMSO): δ=0.93 (t, J=7.1 Hz, 3H), 2.4–2.5 (m, 2H), 3.65 (s, 4H), 3.82 (s, 6H), 3.85 (s, 6H), 6.6–6.7 (m, 4H), 7.24 (d, J=8.3 Hz, 2H), 7.80 ppm (s, 2H); ¹³C NMR (75.5 MHz, [D₆]DMSO): δ=12.2, 50.5, 54.1, 55.4, 55.7, 98.4, 105.3, 116.1, 129.8, 131.2, 131.4, 159.6, 161.8, 186.4 ppm; IR(ATR): ν=2971, 2938, 2837, 2747, 1664, 1597, 1568, 1498, 1454, 1437, 1417, 1308, 1279, 1252, 1207, 1160, 1123, 1094, 1027, 990, 938, 918, 889, 822, 772 cm⁻¹; MS (EI, 70 eV) *m/z* (%): 423 (92) [M⁺], 395 (77), 393 (100), 218 (52), 161 (54).

(*E*)-1-Ethyl-3,5-bis(2,3,4-trimethoxybenzylidene)-4-piperidone x HCl (**2c**). 1-Ethyl-4-piperidone (95 mg, 0.75 mmol) was dissolved in MeOH (5 mL) and 2,3,4-trimethoxybenzaldehyde (294 mg, 1.5 mmol) was added. NaOH (40 mg, 1 mmol) and H₂O (3 mL) were added and the reaction mixture was stirred at room temperature for 3 h. The formed precipitate was collected, washed with MeOH and dried in vacuum. The precipitate was dissolved in CH₂Cl₂ (5 mL), 4 M HCl/dioxane (0.5 mL) was added and the reaction mixture was stirred at room temperature for 5 min. *n*-Hexane was added and the formed precipitate was collected, washed with *n*-hexane and dried in vacuum. Recrystallization from CH₂Cl₂/*n*-hexane gave compound **2c** as a yellow solid (150 mg, 39%): mp: 152–154°C; ¹H NMR (300 MHz, CDCl₃): δ=1.12 (t, J=7.1 Hz, 3H), 2.9–3.0 (m, 2H), 3.85 (s, 6H), 3.88 (s, 6H), 3.89 (s, 6H), 4.3–4.5 (m, 4H), 6.69 (d, J=8.7 Hz, 2H), 6.83 (d, J=8.7 Hz, 2H), 8.27 (s, 2H), 13.0–13.1 ppm (m, 1H); ¹³C NMR (75.5 MHz, CDCl₃): δ=9.8, 46.2, 50.3, 56.1, 60.9, 61.5, 107.3, 119.9, 122.5, 125.4, 140.3, 142.3, 153.4, 156.4, 181.6 ppm; IR(ATR): ν=3396, 2941, 2846, 2445, 1664, 1588, 1493, 1459, 1446, 1415, 1303, 1281, 1230, 1200, 1091, 1051, 1015, 958, 938, 928, 883, 820, 797, 731, 693, 667 cm⁻¹; MS (EI, 70 eV) *m/z* (%): 483 (88) [M⁺], 452 (100).

(*E*)-1-Ethyl-3,5-bis(3-chloro-4,5-dimethoxybenzylidene)-4-piperidone x HCl (**3a**). 1-Ethyl-4-piperidone (95 mg, 0.75 mmol) was dissolved in MeOH (5 mL) and 3-chloro-4,5-dimethoxybenzaldehyde (301 mg, 1.5 mmol) was added. NaOH (40 mg, 1 mmol) and H₂O (1 mL) were added and the reaction mixture was stirred at room temperature for 1 h. The formed precipitate was collected, washed with MeOH and dried in vacuum. The precipitate was dissolved in CH₂Cl₂ (5 mL), 4M HCl/dioxane (0.5 mL) was added and the reaction mixture was stirred at room temperature for 5 min. *n*-Hexane was added and the formed precipitate was collected, washed with *n*-hexane and dried in vacuum. Recrystallization from CH₂Cl₂/*n*-hexane gave compound **3a** as a yellow solid (120 mg, 31%): mp: 124–126°C; ¹H NMR (300 MHz, [D₆]DMSO): δ=1.25 (t, J=7.2 Hz, 3H), 3.3–3.5 (m, 2H), 3.83 (s, 6H), 3.91 (s, 6H), 4.64 (s, 4H), 7.2–7.3 (m, 4H), 7.84 ppm (s, 2H); ¹³C NMR (75.5 MHz, [D₆]DMSO): δ=9.0, 50.2, 56.5, 60.4, 114.6, 123.4, 127.1, 127.3, 130.1, 138.6, 146.0, 153.5, 181.5 ppm; IR(ATR): ν=2940, 2836, 2476, 1677, 1611, 1560, 1490, 1463, 1429, 1413, 1315, 1289, 1253, 1204, 1145, 1049, 995, 942, 852, 810, 770, 750, 730 cm⁻¹; MS (EI, 70 eV) *m/z* (%): 493 (63) [M⁺], 491 (100), 478 (32), 476 (52).

(*E*)-1-Ethyl-3,5-bis(3,5-dichloro-4-methoxybenzylidene)-4-piperidone x HCl (**3b**). 1-Ethyl-4-piperidone (95 mg, 0.75 mmol) was dissolved in MeOH (5 mL) and 3,5-dichloro-4-methoxybenzaldehyde (308 mg, 1.5 mmol) was added. NaOH (40 mg, 1 mmol) and H₂O (1 mL) were added and the reaction mixture was stirred at room temperature for 1 h. The formed precipitate was collected, washed with MeOH and dried in vacuum. The

precipitate was dissolved in CH₂Cl₂ (5 mL), 4 M HCl/dioxane (0.5 mL) was added and the reaction mixture was stirred at room temperature for 5 min. *n*-Hexane was added and the formed precipitate was collected, washed with *n*-hexane and dried in vacuum. Recrystallization from CH₂Cl₂/*n*-hexane gave compound **3b** as a yellow solid (130 mg, 32%): mp: 226–228°C; ¹H NMR (300 MHz, CDCl₃): δ=1.22 (t, J=7.1 Hz, 3H), 3.12 (q, J=7.1 Hz, 2H), 3.92 (s, 6H), 3.93 (s, 6H), 4.4–4.7 (m, 4H), 7.3–7.4 (m, 4H), 7.93 ppm (s, 2H); ¹³C NMR (75.5 MHz, CDCl₃): δ=9.4, 48.2, 49.8, 60.7, 124.8, 130.1, 130.3, 140.8, 153.8, 180.4 ppm; IR(ATR): ν=2938, 2871, 2281, 1683, 1617, 1594, 1542, 1474, 1424, 1407, 1358, 1269, 1254, 1219, 1191, 1147, 1121, 1085, 1042, 1005, 978, 956, 938, 925, 906, 873, 864, 806, 780, 766, 745, 729 cm⁻¹; MS (EI, 70 eV) *m/z* (%): 503 (50) [M⁺], 501 (100), 499 (80), 488 (20), 486 (45), 484 (33).

(*E*)-1-Ethyl-3,5-bis(3-bromo-4,5-dimethoxybenzylidene)-4-piperidone x HCl (**3c**). 1-Ethyl-4-piperidone (95 mg, 0.75 mmol) was dissolved in MeOH (5 mL) and 3-bromo-4,5-dimethoxybenzaldehyde (368 mg, 1.5 mmol) was added. NaOH (40 mg, 1 mmol) and H₂O (1 mL) were added and the reaction mixture was stirred at room temperature for 3 h. The formed precipitate was collected, washed with MeOH and dried in vacuum. The precipitate was dissolved in CH₂Cl₂ (5 mL), 4 M HCl/dioxane (0.5 mL) was added and the reaction mixture was stirred at room temperature for 5 min. *n*-Hexane was added and the formed precipitate was collected, washed with *n*-hexane and dried in vacuum. Recrystallization from CH₂Cl₂/*n*-hexane gave compound **3c** as a yellow solid (150 mg, 32%): mp: 197–198°C; ¹H NMR (300 MHz, [D₆]DMSO): δ=1.24 (t, J=7.2 Hz, 3H), 3.81 (s, 6H), 3.91 (s, 6H), 3.3–3.5 (m, 2H), 4.63 (s, 4H), 7.27 (s, 2H), 7.40 (s, 2H), 7.85 ppm (s, 2H); ¹³C NMR (75.5 MHz, [D₆]DMSO): δ=9.0, 50.4, 56.4, 60.3, 115.2, 117.1, 126.2, 130.8, 138.5, 146.1, 153.3, 181.4 ppm; IR(ATR): ν=2937, 2831, 2362, 1679, 1610, 1588, 1552, 1487, 1464, 1428, 1412, 1314, 1286, 1252, 1201, 1143, 1044, 997, 937, 854, 819, 768, 729 cm⁻¹; MS (EI, 70 eV) *m/z* (%): 583 (52) [M⁺], 581 (100), 579 (50), 568 (22), 566 (43), 564 (23).

(*E*)-1-Ethyl-3,5-bis(3,5-dibromo-4-methoxybenzylidene)-4-piperidone x HCl (**3d**). 1-Ethyl-4-piperidone (95 mg, 0.75 mmol) was dissolved in MeOH (5 mL) and 3,5-dibromo-4-methoxybenzaldehyde (441 mg, 1.5 mmol) was added. NaOH (40 mg, 1 mmol) and H₂O (1 mL) were added and the reaction mixture was stirred at room temperature for 3 h. The formed precipitate was collected, washed with MeOH and dried in vacuum. The precipitate was dissolved in CH₂Cl₂ (5 mL), 4 M HCl/dioxane (0.5 mL) was added and the reaction mixture was stirred at room temperature for 5 min. *n*-Hexane was added and the formed precipitate was collected, washed with *n*-hexane and dried in vacuum. Recrystallization from CH₂Cl₂/*n*-hexane gave compound **3d** as a yellow solid (200 mg, 37%): mp: 198–199°C; ¹H NMR (300 MHz, CDCl₃): δ=1.26 (t, J=7.2 Hz, 3H), 3.0–3.1 (m, 2H), 3.92 (s, 6H), 4.3–4.7 (m, 4H), 7.48 (s, 4H), 7.96 ppm (s, 2H); ¹³C NMR (75.5 MHz, CDCl₃): δ=9.9, 47.5, 49.7, 60.9, 119.2, 124.8, 131.3, 134.0, 141.2, 156.1, 180.6 ppm; IR(ATR): ν=3455, 2928, 2864, 2383, 1679, 1611, 1529, 1469, 1420, 1394, 1252, 1189, 1120, 1067, 1035, 990, 945, 925, 890, 872, 808, 785, 769, 740, 724 cm⁻¹; MS (EI, 70 eV) *m/z* (%): 681 (64) [M⁺], 679 (100), 677 (72), 667 (22), 665 (31), 663 (22).

(*E*)-1-Ethyl-3,5-bis(3-iodo-4,5-dimethoxybenzylidene)-4-piperidone x HCl (**3e**). 1-Ethyl-4-piperidone (64 mg, 0.51 mmol) was dissolved in MeOH (5 mL) and 3-iodo-4,5-dimethoxybenzaldehyde (297 mg, 1.02 mmol) was added. NaOH (40 mg, 1 mmol) and H₂O (1 mL) were added and the reaction mixture was stirred at room temperature for 3 h. The formed precipitate was collected, washed with MeOH and dried in vacuum. The precipitate was dissolved in CH₂Cl₂ (5 mL), 4 M HCl/dioxane (0.5 mL) was added and the reaction mixture was stirred at room temperature for 5 min. *n*-Hexane was added and the formed precipitate was collected, washed with *n*-hexane and dried in vacuum. Recrystallization from CH₂Cl₂/*n*-hexane gave compound **3e** as a yellow solid (120 mg, 33%): mp: 206–208°C; ¹H NMR (300 MHz, CDCl₃): δ=1.25 (t, J=7.2 Hz, 3H), 3.0–3.1 (m, 2H), 3.89 (s, 12H), 4.4–4.6 (m, 4H), 6.82 (s, 2H), 7.31 (s, 2H), 8.03 ppm (s, 2H); ¹³C NMR (75.5 MHz, CDCl₃): δ=10.0, 47.3, 49.9, 56.3, 60.7, 93.1, 114.4, 123.4, 130.7, 132.4, 143.0, 151.1, 152.6, 181.0 ppm; IR(ATR):

FULL PAPER

$\nu=3395, 2935, 2863, 2831, 1356, 1678, 1608, 1583, 1545, 1478, 1464, 1425, 1409, 1309, 1282, 1249, 1200, 1142, 1041, 997, 939, 521, 799, 433, 728, 699, 661 \text{ cm}^{-1}$; MS (EI, 70 eV) m/z (%): 675 (100) [M⁺], 660 (35).

(E)-1-Ethyl-3,5-bis(3,5-diiodo-4-methoxybenzylidene)-4-piperidone x HCl (3f). 1-Ethyl-4-piperidone (66 mg, 0.52 mmol) was dissolved in MeOH (5 mL) and 3,5-diiodo-4-methoxybenzaldehyde (400 mg, 1.03 mmol) was added. NaOH (40 mg, 1 mmol) and H₂O (1 mL) were added and the reaction mixture was stirred at room temperature for 3 h. The formed precipitate was collected, washed with MeOH and dried in vacuum. The precipitate was dissolved in CH₂Cl₂ (5 mL), 4 M HCl/dioxane (0.5 mL) was added and the reaction mixture was stirred at room temperature for 5 min. *n*-Hexane was added and the formed precipitate was collected, washed with *n*-hexane and dried in vacuum. Recrystallization from CH₂Cl₂/*n*-hexane gave compound **3f** as a yellow solid (140 mg, 31%): mp: 193–194 °C; ¹H NMR (300 MHz, [D₆]DMSO): $\delta=1.21$ (t, $J=7.2$ Hz, 3H), 3.2–3.4 (m, 2H), 3.80 (s, 6H), 4.5–4.6 (m, 4H), 7.76 (s, 2H), 7.99 (s, 4H), 11.5–11.6 ppm (m, 1H); ¹³C NMR (75.5 MHz, [D₆]DMSO): $\delta=9.1, 49.9, 60.4, 66.3, 92.1, 127.8, 133.5, 136.8, 141.1, 159.6, 181.4$ ppm; IR(ATR): $\nu=2935, 2323, 1683, 1622, 1593, 1518, 1459, 1412, 1378, 1252, 1187, 1145, 1119, 1058, 1035, 987, 968, 940, 887, 869, 805, 782, 765, 725, 705, 655 \text{ cm}^{-1}$; MS (EI, 70 eV) m/z (%): 867 (100) [M⁺], 852 (20), 142 (69).

Biological evaluation

Cell culture conditions: 518A2 (Department of Radiotherapy, Medical University of Vienna, Austria) melanoma, Panc-1 (ACC-783) pancreatic ductular adenocarcinoma, KB-V1^{vb1} (ACC-149) cervix carcinoma, MCF-7^{Topo} (ACC-115) breast carcinoma, HT-29 (ACC-299), HCT-116 (ACC-581), DLD-1 (ACC-278), SW-480 (CCL-228) colon carcinoma cells were cultivated in Dulbecco's Modified Eagle Medium (DMEM) supplemented with 10% fetal bovine serum, and 1% antibiotic-antimycotic at 37 °C, 5% CO₂, and 95% humidity. To keep MCF-7^{Topo} and KB-V1^{vb1} cells resistant, the maximum-tolerated dose of topotecan or vinblastine were respectively added to the cell culture medium 24 h after every passage. Non-malignant colon epithelial cells (FHC, CRL-1831) were grown in Ham's F12 medium (45%), DMEM (45%), 25 mM HEPES, 10 ng/mL cholera toxin, 0.005 mg/mL insulin, 0.005 mg/mL transferrin, 100 ng/mL hydrocortisone, 10% fetal bovine serum (Sigma Aldrich, St. Louis, MO) and 1% antibiotic-antimycotic solution (Corning, Manassas, VA) at 37 °C in a humidified atmosphere of 5% CO₂. Only mycoplasma-free cell cultures were used.

MTT assay: The assay was performed as described previously.^[35] Briefly, cells (5×10^4 cells/mL, 100 μ L/well) were grown in 96-well plates for 24 h. Then, they were treated with various concentrations of the test compounds, or vehicle (DMSO, or EtOH) for 72 h at 37 °C. After the addition of 12.5 μ L of a 0.5% MTT solution in PBS the cells were incubated for 2 h at 37 °C so that the water-soluble MTT could be converted to formazan crystals. Then, the plates were centrifuged (300 \times g, 5 min, 4 °C), the medium withdrawn, and the formazan dissolved in 25 μ L of DMSO containing 10% SDS and 0.6% acetic acid for at least 2 h at 37 °C. The absorbance of formazan ($\lambda = 570$ nm), and background ($\lambda = 630$ nm) was measured with a microplate reader (Tecan). The IC₅₀ values were derived from dose-inhibition curves as the means \pm SD of four independent experiments with respect to vehicle treated control cells set to 100%.

Hexoseaminidase enzyme assay: To assess proliferation, cells were seeded onto 96-well plates at a density of 5,000 cells per well and allowed to adhere and grow overnight in 10% heat-inactivated FBS containing DMEM. The cells were then treated with increasing doses of the test compounds in 10% FBS containing DMEM. Analysis of cell proliferation was performed by enzymatic assay as described previously.^[36]

DFCH-DA assay: 518A2 melanoma cells (10^5 cells/mL, 50 μ L/well) were grown in a black half-area 96-well plate for 24 h. Then, the medium was exchanged for serum-free DMEM supplemented with 20 μ M DCFH-DA (2',7'-dichlorofluorescein diacetate, Sigma Aldrich) and incubated for 30 min at 37 °C. After washing the cells twice with 100 μ L PBS, 100 μ L of

serum-free DMEM was added. The cells were treated with various concentrations of **2a** and **3c** (0, 1, 5, and 10 μ M) for 1 h at 37 °C. Then, the cells were washed twice with 100 μ L PBS and the plate immediately placed in a microplate reader (TECAN). The DCF fluorescence ($\lambda_{\text{ex}} = 485$ nm; $\lambda_{\text{em}} = 535$ nm) as a measure of intracellular ROS levels was determined and that of untreated control cells was set to 100%. Values exceeding 100% indicate increased ROS concentrations in the cells. The ROS generation (%) was depicted as the mean \pm SD of five independent experiments.

Cell cycle analysis: 518A2 melanoma cells (5×10^4 cells/mL, 3 mL/well) were seeded in 6-well plates and incubated for 24 h. Then, the cells were treated with **2a** (800 nM), **3c** (600 nM), or vehicle (DMSO) for 24 h. After harvesting the cells by trypsination, the cells were fixed with 70% EtOH in water for at least 24 h at 4 °C. Then, cells were pelleted (300 \times g, 5 min, 4 °C), washed with PBS, and stained with PI staining solution (50 μ g/mL propidium iodide, 0.1% sodium citrate, 50 μ g/mL RNase A in PBS) for 30 min at 37 °C. The fluorescence intensity of 10,000 single cells was recorded with a Beckmann Coulter Cytomics FC 500 flow cytometer at $\lambda_{\text{em}} = 630$ nm, and $\lambda_{\text{ex}} = 488$ nm. The percentages of cells in G1, S, and G2/M phase as well as the proportion of apoptotic cells in sub-G1 were analyzed by using the CXP analysis software (Beckmann Coulter).

Gelatin zymography: 518A2 melanoma cells (1×10^5 cells/mL, 3 mL/well) were grown in 6-well plates for 24 h at 37 °C. Then, the medium was aspirated, exchanged for 1.5 mL of cell medium supplemented with 0.1% BSA (bovine serum albumin) and 200 KIU/mL aprotinin and treated with **2a** and **3c** (0, 0.25, 0.5, and 1.0 μ M) for 24 h. After collection of the cell medium containing the secreted proteins, the cells were washed with PBS, and collected by scraping them off in 500 μ L lysis buffer (0.1 M Tris-HCl, 0.2% triton X-100, 200 KIU/mL aprotinin, pH 7.4). For complete lysis cells were first vortexed and then incubated for 20 min on ice. After centrifugation (25,000 \times g, 20 min, 4 °C) the supernatant of medium and cell lysate probes were collected. Equal amount of total protein was subjected to 10% SDS-PAGE co-polymerized with 0.1 mg/mL gelatin. Then, the gels were washed with washing buffer I (50 mM Tris-HCl, 2% triton X-100, pH 7.4) and washing buffer II (50 mM Tris-HCl, pH 7.4) to exchange SDS for triton X-100 so that the partial refolding of proteins was achieved. After incubating the gel for 20 h at 37 °C in MMP assay buffer (50 mM Tris-HCl, 1% triton X-100, 5 mM CaCl₂, pH 7.4), the gels were stained with Coomassie blue and destained until the relevant bands became visible.

Colony formation assay: Briefly, six-well dishes were seeded with 500 HCT-116 cells per well and treated with 0.5 μ M of **2a** or **3c** in 10% fetal bovine serum containing DMEM for 48 h. The compound-containing medium was removed and the cells were incubated for additional 10 days in complete medium to allow colonies to form. The colonies were fixed in formalin followed by staining with crystal violet. Experiments were done in triplicate.

Zebrafish angiogenesis assay: The assay was performed as previously described.^[51] Transgenic animals of the strain *Tg(fli1a:EGFP)* in *t casper* mutant background were raised under standard conditions at 27–28 °C.^[47,48] 24–26 hpf the embryos were manually dechorionated, transferred into 6-well plates [5 embryos/well in 5 mL E3 medium (5 mM NaCl, 0.17 mM KCl, 0.33 mM CaCl₂, 0.33 mM MgSO₄, 0.01% methylene blue, pH 7.2)] and treated with **2a** (5 μ M), **3c** (5 μ M), or vehicle (DMSO) for 48 h. The development of the SIV was documented by fluorescence microscopy ($\lambda_{\text{em}} = 509$ nm, $\lambda_{\text{ex}} = 488$ nm; Leica MZ10F with a ZEISS AxioCam Mrc and the Mrc-ZEN pro 2012 software). The SIV length of at least 17 identically treated embryos was quantified with the ImageJ software and depicted as the mean \pm SD with vehicle treated controls set to 100%. Significant deviations from the control data were determined using a t-test.

Induction of HCT-116 xenografts in mice: Five-week-old male athymic nude mice purchased from Charles River Laboratory were utilized for *in*

FULL PAPER

vivo experiments. They were maintained with water and standard mouse chow ad libitum and used in protocols approved by the University of Kansas Animal Studies Committee. Animals were injected with 1×10^6 HCT116 cells in the left and right flank and allowed to form xenograft. One week following implantation, and after observing the presence of a palpable tumor, **3c** (2 mg/kg body weight mixed with DMSO and 0.5% hydroxypropyl methyl cellulose with 0.1% Tween 80) was administered intraperitoneally daily for 21 d. Tumors were measured weekly. At the end of treatment the animals were euthanized, and the tumors were removed and weighed.

All values are expressed as the mean \pm SEM. Data was analyzed using an unpaired 2-tailed t test. A *P* value of less than 0.05 was considered statistically significant.

Acknowledgements

This work was financially supported by grant 2014-2668-SI-01/1 from Bayern Innovativ, Gesellschaft für Innovation und Wissenschaft mbH (B. Biersack) and by National Institute of Health Grant R01CA190291 and Thomas O'Sullivan Foundation (S. Anant).

Conflict of Interest

The authors declare no conflict of interest.

Keywords: piperidone • halogenation • curcuminoids • angiogenesis • anticancer agents

References:

- [1] R. A. Sharma, S. A. Euden, S. L. Platten, D. N. Cooke, A. Shafayat, H. R. Hewitt, T. H. Marczylo, B. Morgan, D. Hemmingway, S. M. Plummer, M. Pirmohamed, A. J. Gescher, W. P. Steward, *Clin. Cancer Res.* **2001**, *7*, 1894–1900.
- [2] M.H. Pan, T.M. Huang, J. K. Lin, *Drug Metab. Dispos.* **1999**, *27*, 486–494.
- [3] J. M. Reid, S. A. Buhrow, J. A. Gilbert, L. Jia, M. Shoji, J. P. Snyder, M. M. Ames, *Cancer Chemother. Pharmacol.* **2014**, *73*, 1137–1146.
- [4] P. Zou, Y. Xia, W. Chen, X. Chen, S. Ying, Z. Feng, T. Chen, Q. Ye, Z. Wang, C. Qiu, S. Yang, G. Liang, *Oncotarget* **2016**, *7*, 18050–18064.
- [5] D. L. Yin, Y. J. Liang, T. S. Zheng, R. P. Song, J. B. Wang, B. S. Sun, S. H. Pan, L. D. Qu, J. R. Liu, H. C. Jiang, L. X. Liu, *Sci. Rep.* **2016**, *6*, DOI 10.1038/srep32167.
- [6] V. R. Yadav, A. Hussain, J. Xie, S. Kosanke, V. Awasthi, *Scand. J. Trauma Resusc. Emerg. Med.* **2015**, *23:8*, DOI 10.1186/s13049-015-0098-y.
- [7] G. He, C. Feng, R. Vinothkumar, W. Chen, X. Dai, X. Chen, Q. Ye, C. Qiu, H. Zhou, Y. Wang, G. Liang, Y. Xie, W. Wu, *Cancer Chemother. Pharmacol.* **2016**, *78*, 1151–1161.
- [8] F. Thayyullathil, S. Chathoth, A. Hago, M. Patel, S. Galadari, *Free Radic. Biol. Med.* **2008**, *45*, 1403–1412.
- [9] S. Bhaumik, R. Anjum, N. Rangaraj, B. V. V. Pardhasaradhi, A. Khar, *FEBS Lett.* **1999**, *456*, 311–314.
- [10] R. Zhao, L. Tin, Y. Zhang, Y. Wu, Y. Jin, X. Jin, F. Zhang, X. Li, *BioMed Res. Int.* **2016**, DOI 10.1155/2016/8569684.
- [11] X. Tan, N. Sidell, A. Mancini, R. P. Huang, S. Wang, I. R. Horowitz, D. C. Liotta, R. N. Taylor, F. Wieser, *Reprod. Sci.* **2010**, *17*, 931–940.
- [12] D. Subramaniam, R. May, S. M. Sureban, K. B. Lee, R. George, P. Kuppasamy, R. P. Ramanujam, K. Hideg, B. K. Dieckgraefe, C. Houchen, S. Anant, *Cancer Res.* **2008**, *68*, 1962–1969.
- [13] M. Shen, M. Y. Wu, L. P. Chen, Q. Zhi, F. R. Gong, K. Chen, D. M. Li, Y. Wu, M. Tao, W. Li, *Sci. Rep.* **2015**, *5*, DOI 10.1038/srep11836.
- [14] B. K. Adams, E. M. Ferstl, M. C. Davis, M. Herold, S. Kurtkaya, R. F. Camalier, M. G. Hollingshead, G. Kaur, E. A. Sausville, F. R. Rickles, J. P. Snyder, D. C. Liotta, M. Shoji, *Bioorg. Med. Chem.* **2004**, *12*, 3871–3883.
- [15] L. Cen, B. Hutzen, S. Ball, S. DeAngelis, C. L. Chen, J. R. Fuchs, C. Li, P. K. Li, J. Lin, *BMC Cancer* **2009**, *9:99*, DOI 10.1186/1471-2407-9-99.
- [16] P. C. Leow, P. Bahety, C. P. Boon, C. Y. Lee, K. L. Tan, T. Yang, P. L. R. Ee, *Eur. J. Med. Chem.* **2014**, *71*, 67–80.
- [17] S. Manohar, S. I. Khan, S. K. Kandi, K. Raj, G. Sun, X. Yang, A. D. C. Molina, N. Ni, B. Wang, D. S. Rawat, *Bioorg. Med. Chem. Lett.* **2013**, *23*, 112–116.
- [18] A. Brown, Q. Shi, T. W. Moore, Y. Yoon, A. Prussia, C. Maddox, D. C. Liotta, H. Shim, J. P. Snyder, *J. Med. Chem.* **2013**, *56*, 3456–3466.
- [19] M. Yamaguchi, T. W. Moore, A. Sun, J. P. Snyder, M. Shoji, *Integr. Biol.* **2012**, *4*, 905–913.
- [20] M. Helal, U. Das, B. Bandy, A. Islam, A. J. Nazarali, J. R. Dimmock, *Bioorg. Med. Chem. Lett.* **2013**, *23*, 1075–1078.
- [21] A. Thakur, S. Manohar, C. E. V. Gerena, B. Zayas, V. Kumar, S. V. Malhotra, D. S. Rawat, *Med. Chem. Commun.* **2014**, *5*, 576–586.
- [22] K. L. Tan, A. Ali, Y. Du, H. Fu, H. X. Jin, T. M. Chin, M. Khan, M. L. Go, *J. Med. Chem.* **2014**, *57*, 5904–5918.
- [23] F. Schmitt, M. Gold, G. Begemann, I. C. Andronache, B. Biersack, R. Schobert, *Bioorg. Med. Chem.* **2017**, *25*, 4894–4903.
- [24] G. R. Pettit, S. B. Singh, E. Hamel, C. M. Lin, D. S. Alberts, D. Garcia-Kendall, *Cell. Mol. Life Sci.* **1989**, *45*, 209–211.
- [25] J. L. Hartwell, A. W. Schrecker, *J. Am. Chem. Soc.* **1951**, *73*, 2909–2916.
- [26] Geiger, P. L. *Eur. J. Org. Chem.* **1833**, *7*, 269–280.
- [27] B. Yadav, S. Taurin, R. J. Rosengren, M. Schumacher, M. Diederich, T. J. Somers-Edgar, L. Larsen, *Bioorg. Med. Chem.* **2010**, *18*, 6701–6707.
- [28] S. Das, U. Das, D. Michel, D. K. J. Gorecki, J. R. Dimmock, *Eur. J. Med. Chem.* **2013**, *64*, 321–328.
- [29] F. A. M. Al-Omary, G. S. Hassan, S. M. El-Messery, H. I. El-Subbagh, *Eur. J. Med. Chem.* **2012**, *47*, 65–72.
- [30] D. M. Lonard, L. Wang, B. W. O'Malley, J. Xu, Y. Song, X. Li, T. G. Palzkill (Baylor College of Medicine, Houston, TX, USA), Int. PCT Pub. No. WO 2016/109470 A1, **2016**.
- [31] K. Youssef, M. A. El-Sherbeny (Fish & Neave IP Group Ropes & Gray LLP, Boston, MA, USA), US Pub. No.: US 2007/0010488 A1, **2007**.
- [32] J. Chen, L. Zhang, Y. Shu, L. Chen, M. Zhu, S. Yao, J. Wang, J. Wu, G. Liang, H. Wu, W. Li, *BioMed Res. Int.* **2017**, DOI 10.1155/2017/4751260.
- [33] B. Biersack, Y. Muthukumar, R. Schobert, F. Sasse, *Bioorg. Med. Chem. Lett.* **2011**, *21*, 6270–6273.
- [34] R. Schobert, B. Biersack, A. Dietrich, K. Effenberger, S. Knauer, T. Mueller, *J. Med. Chem.* **2010**, *53*, 6595–6602.
- [35] T. Mosmann, *J. Immunol. Methods* **1983**, *65*, 55–63.
- [36] U. Landegren, *J. Immunol. Methods* **1984**, *67*, 379–88.
- [37] A. T. Y. Lau, Y. Wang, J. F. Chiu, *J. Cell. Biochem.* **2008**, *104*, 657–667.
- [38] P. Zou, Y. Xia, W. Chen, X. Chen, S. Ying, Z. Feng, T. Chen, Q. Ye, Z. Wang, F. Qiu, *Oncotarget* **2016**, *7*, 18050–18064.
- [39] C. Gialeli, A. D. Theocharis, N. K. Karamanos, *FEBS J.* **2011**, *278*, 16–27.
- [40] J. K. Muenzner, B. Biersack, H. Kalie, I. C. Andronache, L. Kaps, D. Schuppan, F. Sasse, R. Schobert, *ChemMedChem* **2014**, *9*, 1195–1204.
- [41] U. B. Hofmann, J. R. Westphal, G. N. Van Muijen, D. J. Ruiter, *J. Invest. Dermatol.* **2000**, *115*, 337–344.
- [42] P. A. Snoek-van Beurden, J. W. Von den Hoff, *Biotechniques* **2005**, *38*, 73–83.
- [43] Y. Qian, P. Zhong, D. Liang, Z. Xu, M. Skibba, C. Zeng, X. Li, T. Wei, L. Wu, G. Liang, *PLoS ONE* **2015**, *10*, DOI 10.1371/journal.pone.0120215.
- [44] A. Mitra, J. Chakrabarti, A. Banerji, A. Chatterjee, B. R. Das, *J. Environ. Pathol. Toxicol. Oncol.* **2006**, *25*, 679–690.
- [45] G. N. Serbedzija, E. Flynn, C. E. Willett, *Angiogenesis* **1999**, *3*, 353–359.
- [46] S. Isogai, M. Horiguchi, B. M. Weinstein, *Dev. Biol.* **2001**, *230*, 278–301.
- [47] N. D. Lawson, B. M. Weinstein, *Dev. Biol.* **2002**, *248*, 307–318.
- [48] R. M. White, A. Sessa, C. Burke, T. Bowman, J. LeBlanc, C. Ceol, C. Borque, M. Dovey, W. Goessling, C. E. Burns, L. I. Zon, *Cell Stem Cell* **2008**, *2*, 183–189.
- [49] P. Lagisetty, D. R. Powell, V. Awasthi, *J. Mol. Struct.* **2009**, *936*, 23–28.

FULL PAPER

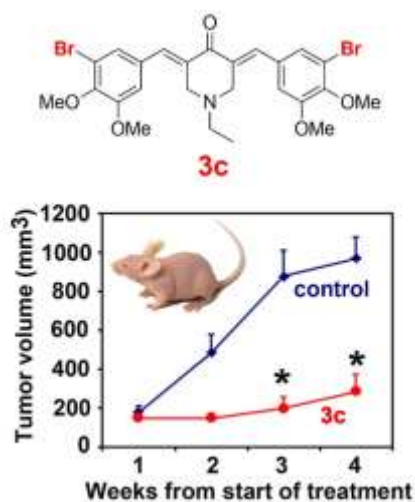
- [50] Y. Wang, X. Shan, Y. Dai, L. Jiang, G. Chen, Y. Zhang, Z. Wang, L. Dong, J. Wu, G. Guo, G. Liang, *J. Pharmacol. Exp. Ther.* **2015**, *353*, 539–550.
- [51] H. Draut, T. Rehm, G. Begemann, R. Schobert, *Chem. Biodivers.* **2017**, *14*, DOI 10.1002/cbdv.201600302.

WILEY-VCH

Accepted Manuscript

FULL PAPER

Entry for the Table of Contents



The curcumin halo effect: The new 3-bromo-4,5-dimethoxyphenyl curcuminoid **3c** showed higher antiproliferative activity than the known fluoro-curcuminoid EF24. **3c** revealed great potential as promising anticancer drug candidate due to its superior antiproliferative, ROS-inducing, and anti-invasive activity as well as its strong tumor growth inhibitory activity in HCT-116 mouse xenografts.